Hayami Kawamoto[1]
Naoki Higashitarumizu[1], Masaru Nakamura[2], Itsuki Yonemori[3],
Katsunori Wakabayashi[3], and Kosuke Nagashio[1]
[1]Department of Materials Engineering, The University of Tolyo, 7-3-1 Hongo, Tokyo 113-8656, Japan
[2]National Institute for Materials Science, 1-1 Namiki, Tsukuba, Ibaraki 305-0044, Japan
[3]Department of Nanotechnology for Sustainable Energy, Kwansei Gakuin University, Gakkuen 2-1, Sanda, Hyogo 669-1337, Japan

kawamoto@ncd.t.u-tokyo.ac.jp

Growth and Characterization of High Quality Monolayer SnS

Self-sufficient energy harvesting is the urgent issue for continuously increasing IoT sensors. Since monolayer SnS has been theoretically predicted as the piezoelectric material with high piezoelectric coefficient comparable to that of PZT [1], the physical vapor deposition (PVD) growth of SnS has been competitively investigated be-cause the flexibility of 2D overcomes the disadvantage of brittleness for PZT. Monolayer SnS, however, has not been realized yet [2], because the ionic bonding due to the lone pair electrons as well as van der Waals bonding strengthens the interlayer interaction, resulting in the easy growth of multilayer SnS. So far, PVD growth of SnS with several 100 nm in thickness has been investigated as Pb-free solar cells [3] and thermoelectric materials [4]. The common problem has been pointed out as the impurities in source powders, i.e., Sn2S3, SnOx and so on. However, despite that the impurities are expected to largely affect the PVD growth of monolayer SnS, it has not been elucidated yet. In this study, in addition to the purchased SnS powder, the high purity SnS crystal grown from distillated S and Sn shot (99.99%) is used as source material [5]. As shown in **Figure. 1**, the impurities are not detected by the powder X-ray diffraction. By comparing the initial stage of the growth, the approach to grow the high quality monolayer SnS is discussed.

The tube furnace with 3-zone heaters was used for the PVD growth, where the temperatures for source powders and mica substrates were controlled independently. Mica substrate with atomically flat surface was initially heated and maintained at the target temperature and, then, source powders were heated. After growth, heater was opened immediately and cooled rapidly. The grown flakes were characterized by atomic force microscopy (AFM) and Raman spectroscopy.

First of all, the SnS growth from high purity crystal is discussed. After the growth, thin SnS flakes with clear rhombus shape were obtained on mica without any detectable additional grains, as shown in **Figure 2(a)**. However, even after the various growth conditions were tested, their thickness was not thinner than 2.0 nm which is thicker than monolayer (~0.6 nm). Moreover, although Raman peak was detected for 2.6-nm-thick SnS, it disappeared for 2.0-nm-SnS, as shown in **Figure 2(b)**, suggesting the poor crystallinity.

On the other hand, for purchased powder including impurities, the circular shape SnS with ~0.8 nm in thickness was obtained on mica with small additional grains, as shown in **Figure 3(a)**, which is approximately monolayer thickness. **Figure 3(b)** shows the Raman spectra of SnS with different thickness from 20 nm to ~0.8 nm. Peak shift with decreasing the thickness is consistent with the first principle calculation shown in **Figure 4**. Even for monolayer thick SnS, Raman peak was detected, suggesting the better crystallinity. However, peak around 150 cm-1 disappeared at monolayer thickness. To further find out the lost peak, polarized Raman spectroscopy was conducted for the monolayer thick SnS. The two separated peaks at ~130 and ~155 cm-1 were clearly detected at specific rotation angle due to the strong anisotropic crystal structure, as shown in **Figure 5**, which is again consistent with the first principle calculation. These data clearly indicate the successful PVD growth of monolayer SnS from purchased powders including impurities.

Compared with the growth from high purity SnS crystal, there are many small grains around the monolayer SnS. To identify whether these grains are SnS or not, re-evaporation experiment was conducted at the temperature higher than that for the growth (400˚C, 20 min.). **Figure 3(b)** shows the before/after the re-

evaporation. The SnS flake disappears after re-evaporation, while the grains around and under the flake still remain. This indi-cates that these grains are not SnS. Moreover, Auger electron spectroscopy suggests the grains are S-rich compound. These results suggest that grains are grown from impurities in the source powders and that these grains could play important role in the monolayer SnS growth.

Finally let's discuss the growth mechanism of mono-layer SnS. In case of the high purity SnS source, SnS grows on the atomically flat mica substrate. Due to the lone pair electrons, however, it is more likely to grow perpendicularly instead of horizontally. This leads to the flakes with thicker than 2.0 nm. But for the source with impurities, monolayer SnS was obtained. Because Sn2S3, impurity in the source powder, is initially evaporated due to lower melting point, S-rich condition could be attained at the mica surface, leading the change in its wettability. Therefore, under this condition, the horizontal growth is more likely than perpendicular growth, resulting in the growth of monolayer SnS.

Monolayer SnS flake was successfully grown from the source powders including impurities. By comparing the growth results obtained by different source materials, the S-rich condition on mica substrate could be the key to achieve the horizontal growth. By using high purity SnS source material with additional S powder, the precisely controlled growth of monolayer SnS might be realized.

References

[1] R. Fei, *et al.*, *Appl. Phys. Lett.*, 2015, **107**, 173104.
[2] J. Xia, *et al., Nanoscale,* 2016, **8**, 2063.
[3] P. Sinsermsuksakul, *et al., Adv. Energy Mater.,* 2014, **4**, 1400496.
[4] Q. Tan, *et al., J. Mater. Chem. A,* 2014, **2**, 17302.
[5] M. Nakamura, *et al., J. Alloys Comp.,* 2014, **591**, 326.

Figures

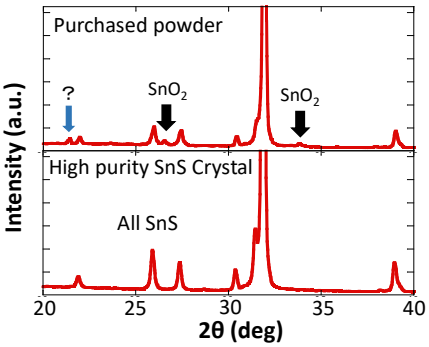

Figure 1:XRD of powder and high purity grown crystal, respectively. The crystal was grinded into powders for the measurement.

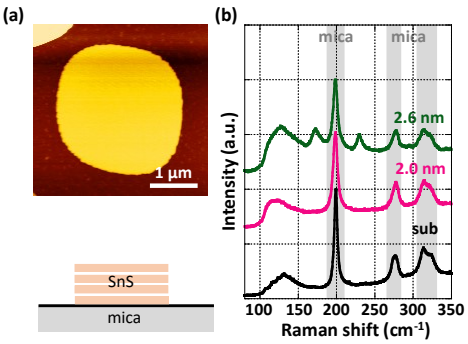

Figure 2:(a)AFM image of SnS grown from high purity crystal source and schematic illustration of its cross section. (b) Raman spectra of SnS grown from high purity crystal source.

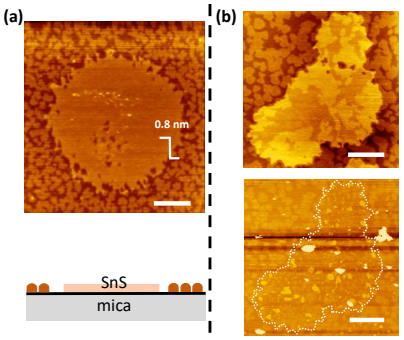

Figure 3:(a)AFM image of SnS grown from powder source and schematic illustration of its cross section. (b) AFM images of before/after the re-evaporation experiment. Each scale bar indicates 1 μm.

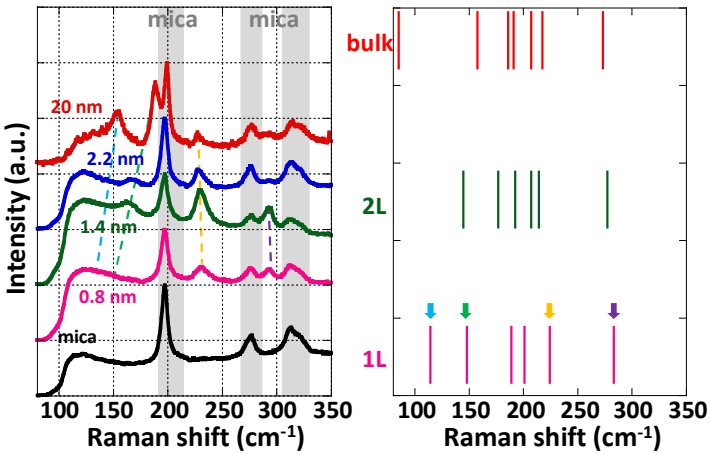

Figure 4: Raman spectra of SnS grown from powder with different thickness and the results from first principle calculation.

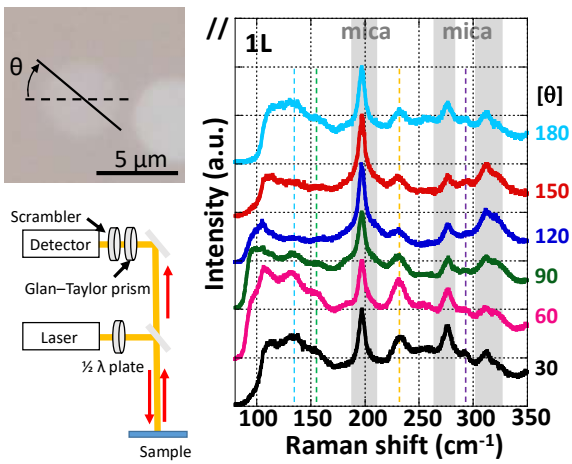

Figure 5: Polarized Raman spectra of monolayer SnS. 1/2 λ plate and Glan-Taylor prism were placed in parallel.